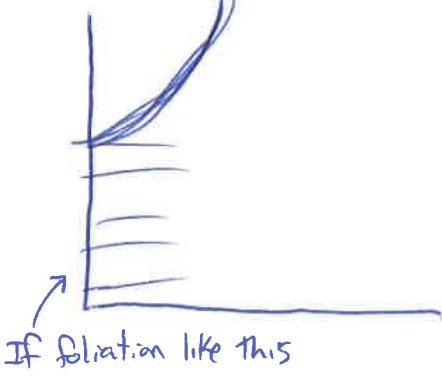


Zenginoglu

Fig 1.

blowup profile.



HYPERBOLOIDAL EVOLUTION AND APPLICATIONS

ANIL ZENGINOĞLU

For his pictures, blue is null, red is timelike and green is spacelike.

Hyperboloidal slide: It is easier to take one hyperboloid and then shift along the Killing field, like the 2nd picture.

Wave equations slide: In Penrose diagrams, it becomes clear that energy from radiation is in any slice of an AF slicing, but it eventually leaves a AH slicing.

Blow-up ($b < 0$) slide: See figure 1: If taking an AF foliation, we see blow up at origin. If a hyperboloidal foliation, and steeper than the blowup profile, we see it at infinity. If the hyperboloidal foliation is at just the right steepness, you can get blowup everywhere on a slice.

Does this method work for elliptic equations (for GR)? It seems to work well for the CMC foliation formulation of the Einstein equations, but not so well for free evolution formulation right now.

Hyperboloidal evolution and applications

Anıl Zenginoğlu

California Institute of Technology

MSRI, Berkeley, November 19, 2013



Overview

Introduction

Hyperboloidal surfaces

Advantages

Energy decay; Outer boundary; Asymptotic solution; Negative cost

Cubic wave equation

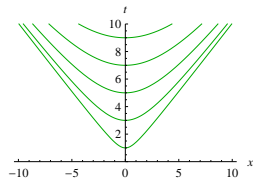
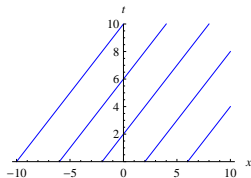
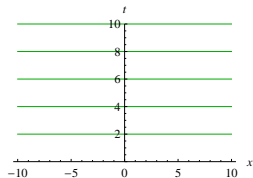
Scalar Green functions

Quasi-normal modes



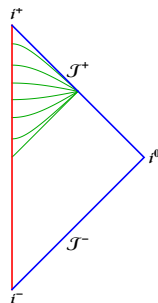
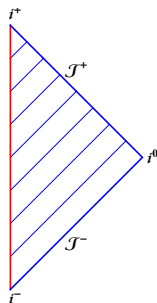
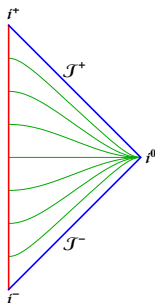
Hyperboloidal evolution

Dirac (1949) distinguishes three "forms" of quantum field theory:
 instant (**Cauchy**), light front (**characteristic**), and point (**hyperboloidal**).



Hyperboloidal evolution

Dirac (1949) distinguishes three "forms" of quantum field theory:
 instant (**Cauchy**), light front (**characteristic**), and point (**hyperboloidal**).



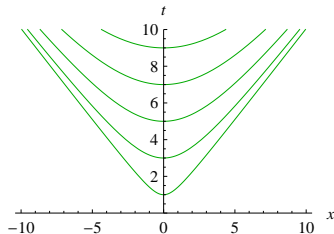
Hyperboloidal surfaces

In a spacetime with metric $g_{\mu\nu}$ and coordinates x^μ a **hyperboloid** is defined by

$$-g_{\mu\nu}x^\mu x^\nu = \tau^2, \quad \tau \neq 0$$

In two dimensional flat spacetime with coordinates (t, x)

$$t^2 - x^2 = \tau^2.$$



Hyperboloids to Lorentzian geometry are like spheres to Riemannian geometry.

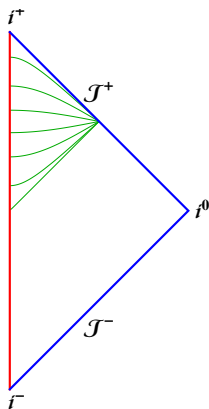
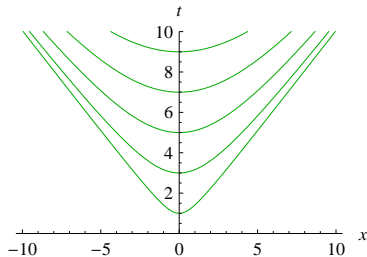


Hyperboloidal surfaces

A surface is called hyperboloidal (Friedrich 1983) iff

- it is spacelike, and
- it approaches null infinity.

$$t^2 - x^2 = \tau^2 \Rightarrow \partial_t = \frac{\sqrt{\tau^2 + x^2}}{\tau} \partial_\tau.$$

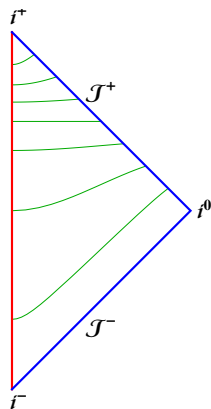
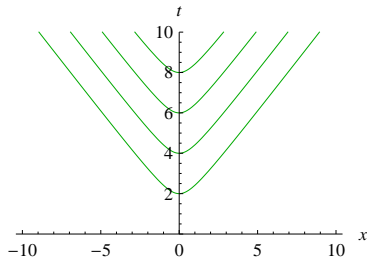


Hyperboloidal surfaces

A surface is called hyperboloidal (Friedrich 1983) iff

- it is spacelike, and
- it approaches null infinity.

$$(t - \tau)^2 - x^2 = 1 \Rightarrow \partial_t = \partial_\tau.$$



Wave equations

Consider the semi-linear wave equation

$$(-\partial_t^2 + \Delta_x)u(t, x) \pm |u(t, x)|^{p-1}u(t, x) = 0, \quad x \in \mathbb{R}^3.$$

Two properties that seem to contradict intuition:

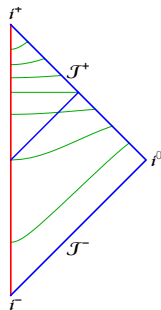
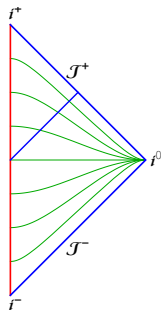
- Time-reversibility: $t \rightarrow -t$ is a symmetry.
- Conservation of energy: $\partial_t E(u) = 0$ with

$$E(u) = \int_0^\infty \frac{1}{2} \left((\partial_t u)^2 + |\nabla_x u|^2 \pm \frac{1}{p+1} u^{p+1} \right) dx.$$



Wave equations

Compare Penrose diagrams



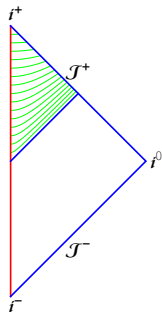
Wave equations

As an example for a hyperboloidal foliation, consider the Kelvin inversion

$$x^\mu = -\frac{X^\mu}{X_\nu X^\nu},$$

$$t = -\frac{T}{T^2 - |X|^2}, \quad x^i = \frac{X^i}{T^2 - |X|^2}.$$

The domain is $|X| < -T$, $T \in (-\infty, 0)$.



The wave equation $u_{tt} - u_{rr} = 0$ becomes $u_{TT} - u_{RR} = 0$. The energy

$$E(u) = \int_0^{-T} \frac{1}{2} (u_T(T, R)^2 + u_R(T, R)^2) dR,$$

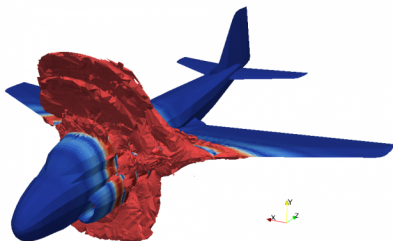
decays in time

$$\frac{\partial E}{\partial T} = -\frac{1}{2} (u_T(T, -T) - u_R(T, -T))^2 \leq 0.$$



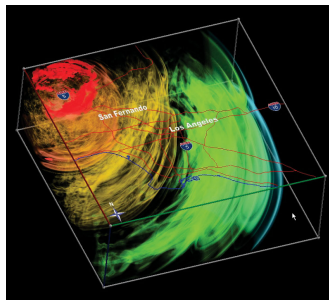
Numerical calculations

Maxwell equations



Electromagnetic scattering off a plane
(Andreas Kloeckner, Courant Institute).

Seismic wave equation.



1994 Northridge Earthquake
(Quake Project, Carnegie Mellon).

The outer boundary problem

To solve the initial value problem numerically, one truncates the unbounded domain because: “Compactification is **not compatible** with hyperbolic PDEs.”

The resulting artificial outer boundary is not part of the physical problem. To make sure that the truncated solution approximates the original solution:

- The boundary *conditions* must lead to a **well-posed** initial boundary value problem, and possibly preserve constraints.
- The boundary *data* must be **transparent** to physics.
- The numerical *implementation* should be **stable, accurate, and efficient**.

⇒ Extensive research for many decades

- ABC: Absorbing boundary conditions (Engquist–Majda 1977).
- PML: Perfectly matched layer (Bérenger 1994).



The compactification problem

Compactification refers to the mapping of an **infinite physical domain** to a **finite computational domain** by a coordinate transformation. For example, consider

$$\rho = \frac{x}{1+x}, \quad x = \frac{\rho}{1-\rho} \equiv \frac{\rho}{\Omega}.$$

The compactifying coordinate ρ maps the infinitely extended domain $[0, \infty)$ onto the bounded domain $[0, 1)$.

The function $\Omega(\rho)$ vanishes at infinity with non-vanishing gradient.



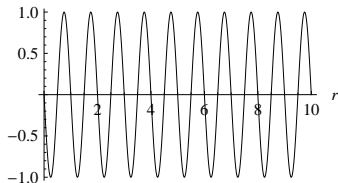
The compactification problem

Consider the outgoing sine-wave solution

$$u(t, x) = \sin(x - t).$$

at $t = 0$ we have

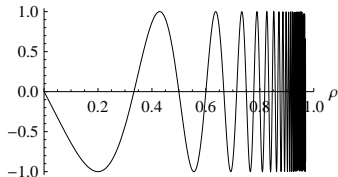
$$u(0, x) = \sin x.$$



Compactification $x = \rho/\Omega$ leads to

$$u_0 = \sin(\rho/\Omega).$$

Infinite oscillations cannot be resolved on a finite domain.

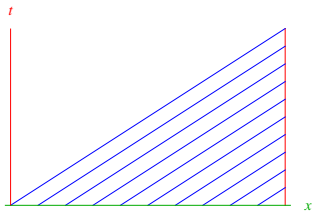


The compactification problem

Consider the advection equation

$$\partial_t u + \partial_x u = 0$$

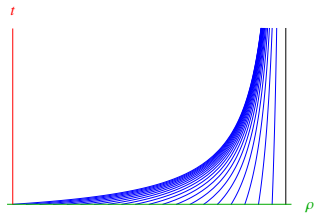
Characteristics leave the domain through a timelike boundary.



Compactification leads to

$$\partial_t u + \Omega^2 \partial_\rho u = 0.$$

Characteristics are trapped.



Solution: Hyperboloidal compactification

Introduce a new **time coordinate** τ in addition to compactification such that the outgoing characteristic has the same form in compactifying coordinates.

$$t - x = \tau - \rho.$$



Henceforth space by itself, and time by itself, are doomed to fade away into mere shadows, and only a kind of union of the two will preserve an independent reality.

Hermann Minkowski 1908

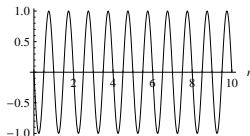


Hyperboloidal compactification

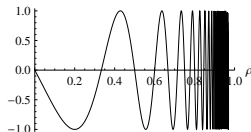
To avoid loss of resolution near the domain boundaries, introduce τ such that

$$\tau - \rho = t - x$$

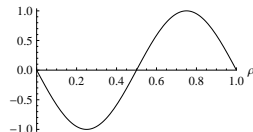
Given ρ , the above relation defines the time function τ .



$$\sin(t - x)$$



$$\sin\left(t - \frac{\rho}{\Omega}\right)$$



$$\sin(\tau - \rho)$$

Advection equation

The Jacobian of the hyperboloidal compactification reads

$$\partial_\tau = \partial_t, \quad \partial_x = (-1 + \Omega^2)\partial_\tau + \Omega^2 \partial_\rho.$$

The advection equation transforms as $\partial_t u + \partial_x u = \Omega^2 (\partial_\tau u + \partial_\rho u)$. We get

$$\partial_t u + \partial_x u = 0 \quad \Rightarrow \quad \partial_\tau u + \partial_\rho u = 0.$$

The equation is the same but the meaning of the coordinates is different.



Wave equation

The wave equation in $x \in (-\infty, \infty)$ becomes in $\rho \in [-1, 1]$

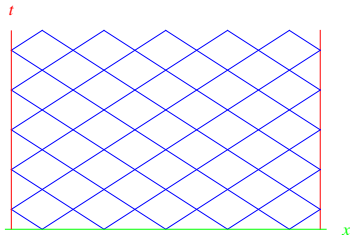
$$-(1 + H)\partial_\tau^2 u - 2H\partial_\tau\partial_\rho u + \Omega^2\partial_\rho^2 u + 2\Omega\partial_\rho\Omega(\partial_\tau + \partial_\rho)u = 0,$$

where $H(\rho)$ is a function that satisfies $H(\pm 1) = \pm 1$.

We get at infinity

$$\partial_\tau(\partial_\tau u \pm \partial_\rho u) = 0.$$

There are no incoming characteristics into the computational domain.



$$\square_{tx} u = 0$$



Wave equation

The wave equation in $x \in (-\infty, \infty)$ becomes in $\rho \in [-1, 1]$

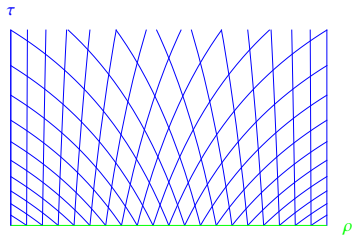
$$-(1 + H)\partial_\tau^2 u - 2H\partial_\tau\partial_\rho u + \Omega^2\partial_\rho^2 u + 2\Omega\partial_\rho\Omega(\partial_\tau + \partial_\rho)u = 0,$$

where $H(\rho)$ is a function that satisfies $H(\pm 1) = \pm 1$.

We get at infinity

$$\partial_\tau(\partial_\tau u \pm \partial_\rho u) = 0.$$

There are no incoming characteristics into the computational domain.

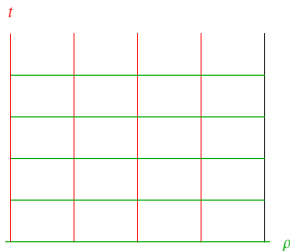
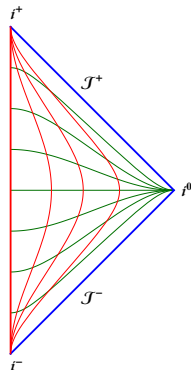


$$\square_{\tau\rho} u = 0$$



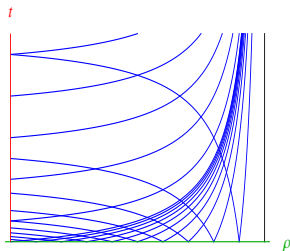
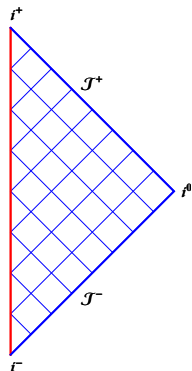
Penrose diagrams

Hyperboloidal compactification and the resulting characteristic structure can be visualized in a Penrose diagram.



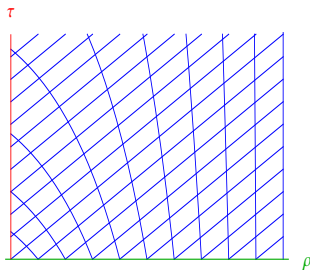
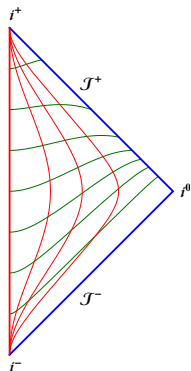
Penrose diagrams

Hyperboloidal compactification and the resulting characteristic structure can be visualized in a Penrose diagram.



Penrose diagrams

Hyperboloidal compactification and the resulting characteristic structure can be visualized in a Penrose diagram.



Summary

Hyperboloidal compactification

- makes energy decay explicit,
- avoids contamination by artificial boundary conditions,
- provides the unbounded domain solution,
- at negative cost (computational efficiency factors 100–5000).

Disadvantages:

- Equations “look” more complicated (no unitary evolution).
- No access to spatial infinity (solutions are semi-global).



The focusing cubic wave equation

Piotr Bizoń and AZ, *Nonlinearity* 2009.

Consider the semilinear wave equation in Minkowski spacetime with a focusing cubic nonlinearity,

$$\partial_{tt}v - \Delta v = v^3.$$

- Global existence for small data:
Decay as t^{-2} near i^+ , as t^{-1} along \mathcal{I}^+ as $t \rightarrow \infty$.

Christodoulou 1986

- Blowup for large data:
The blowup mechanism is ODE-blowup.

$$\partial_{tt}v = v^3, \quad v(T) = \infty \quad \rightarrow \quad v = \frac{\sqrt{2}}{T-t}.$$

Merle & Zaag 2005, Donninger & Schörkhuber 2012.



The symmetry orbit

The cubic wave equation admits the following symmetries

- time translation, $T_a : v(t, r) \rightarrow v(t + a, r)$
- conformal inversion, $I : v(t, r) \rightarrow \frac{1}{t^2 - r^2} v\left(\frac{t}{r^2 - t^2}, \frac{r}{t^2 - r^2}\right)$,
- reflection, $v \rightarrow -v$.

The symmetry orbit of the solution $\pm\sqrt{2}/t$ is obtained from $T_a I T_b$

$$\pm v_{(a,b)}(t, r) = \pm \frac{\sqrt{2}}{t + a + b((t + a)^2 - r^2)}.$$

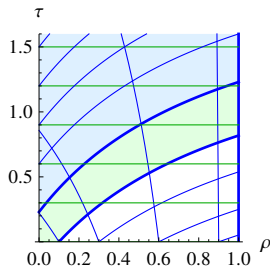
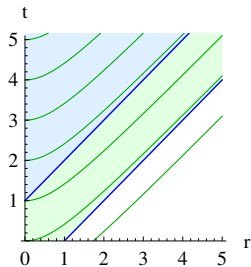
Conjecture: This two parameter family of solutions acts as a local attractor for a large set of spherically symmetric data.

The sign of b determines the nature of solution (decay, blow-up, criticality).



Decay ($b > 0$)

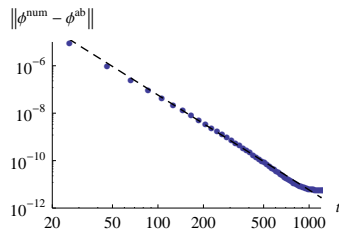
Convergence to the attractor is expected beyond the evolution of initial data.



Decay ($b > 0$)

Linear stability analysis indicates

$$v_{\text{generic}} - v_{(a,b)} = \frac{C}{t^4} + \mathcal{O}(t^{-5}).$$



Blow-up ($b < 0$)

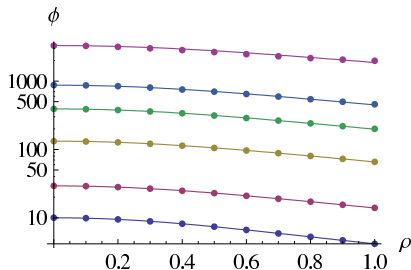
The blow-up profile is a hyperboloidal surface given by

$$t = \left(\frac{1}{2|b|} - a \right) + \sqrt{\frac{1}{4b^2} + r^2}.$$

In this work, we used hyperboloidal coordinates defined through

$$t = \tau + \sqrt{1 + r^2}.$$

Simultaneous blowup on each grid point for $b = -\frac{1}{2}$.

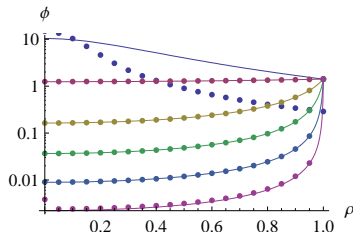


The critical solution ($b = 0$)

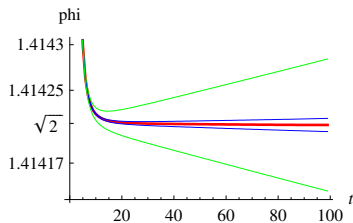
We expect the critical solution to be

$$v_0(t, x) = \frac{\sqrt{2}}{t}.$$

The field at null infinity for the critical solution is $\sqrt{2}$.



The numerical solution compared with the attractor solution at times $\tau = \{3, 5, \dots, 1280\}$.



The difference $b - b_*$ is $\pm 10^{-9}$ for blue curves, $\pm 10^{-8}$ for green curves.



Nondispersive decay

Roland Donniger and AZ, *Analysis & PDE* 2014.

Theorem

There exists a co-dimension 4 Lipschitz manifold \mathcal{M} of functions in $H^1(\Sigma_{-1}) \times L^2(\Sigma_{-1})$ with $(0, 0) \in \mathcal{M}$ such that the following holds. For data $(f, g) \in \mathcal{M}$ the hyperboloidal initial value problem

$$\begin{cases} (-\partial_t^2 + \Delta_x)v(t, x) + v(t, x)^3 = 0 \\ v|_{\Sigma_{-1}} = v_0|_{\Sigma_{-1}} + f \\ \nabla_n v|_{\Sigma_{-1}} = \nabla_n v_0|_{\Sigma_{-1}} + g \end{cases}$$

has a unique solution v defined on $D^+(\Sigma_{-1})$ such that

$$|T|^{\frac{1}{2}} \left(\|v - v_0\|_{H^1(\Sigma_T)} + \|\nabla_n v - \nabla_n v_0\|_{L^2(\Sigma_T)} \right) \lesssim |T|^{\frac{1}{2}-}$$

for all $T \in [-1, 0)$. As a consequence, for any $\delta \in (0, 1)$, we have

$$\|v - v_0\|_{L^4(t, 2t)L^4(B_{(1-\delta)t})} \lesssim t^{-\frac{1}{2}+}$$

as $t \rightarrow \infty$, i.e., v converges to v_0 in a localized Strichartz sense.



The hyperboloidal initial value problem

The hyperboloidal surfaces Σ_T are defined via

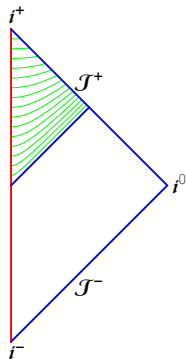
$$\Sigma_T := \left\{ (t, x) \in \mathbb{R} \times \mathbb{R}^3 : t = -\frac{1}{2T} + \sqrt{\frac{1}{4T^2} + |x|^2} \right\}, \text{ where } T \in (-\infty, 0).$$

The transformation $(t, x) \mapsto (T, X)$

$$T = -\frac{t}{t^2 - |x|^2}, \quad X = \frac{x}{t^2 - |x|^2}$$

maps the forward lightcone $\{|x| < t, t > 0\}$ to the backward lightcone $\{|X| < -T, T < 0\}$, and $t \rightarrow \infty$ translates into $T \rightarrow 0^-$.

The problem translates into the stability of the blow-up solution in the backward lightcone of the origin (Donninger & Schörkhuber 2012).



The Green function as the fundamental solution

AZ and Chad Galley, *Physical Review D* 2012.

Given a linear partial differential equation, its **Green function** (*fundamental solution*) provides a complete description.

For example, the Green function for the scalar wave operator \square satisfies

$$\square G(x, x') = \delta^4(x - x')$$

with appropriate boundary conditions. The inhomogeneous equation

$$\square \phi(x) = S(x),$$

can be solved via the Green function by a simple convolution

$$\phi(x) = \int G(x, x') S(x') d^4 x',$$

A similar procedure applies to non-vanishing initial data.



Features of curved spacetime Green functions

There are three main features that make the construction of a curved spacetime Green function a difficult problem:

1. Backscatter off curvature propagates **within** the lightcone.
2. Light cone intersects itself along **caustics**.
3. A source encounters its own echoes due to **trapping at the photon sphere**.

There has been considerable effort to construct the retarded Green function through matched asymptotic expansions (Anderson, Flanagan, Hu, Ottewill, Poisson, Wiseman 1999–2005), but the problem remained unsolved.



Global evolution of local perturbations

An approximation to the Green function can be obtained numerically by solving

$$\square\phi_\sigma(x; x') = \frac{1}{(\sqrt{2\pi}\sigma)^4} \exp\left[-\frac{(x - x')^2}{2\sigma^2}\right]$$

with a finite σ . This is a problem with three scales:

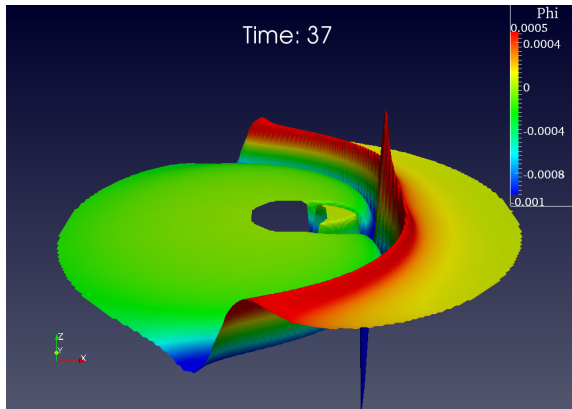
- The scale of the Gaussian σ .
- The scale of the black hole M .
- The scale of the ideal observer ∞ .

This is a multi scale problem (computational high frequency wave propagation). Hyperboloidal compactification solves the large scale.



The simulation

For the simulations we used **SpEC** on an **infinite** domain.



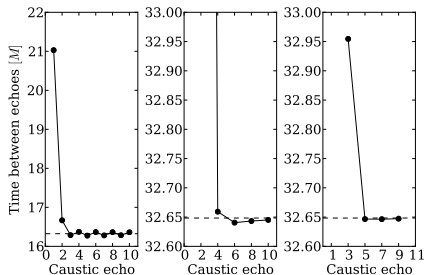
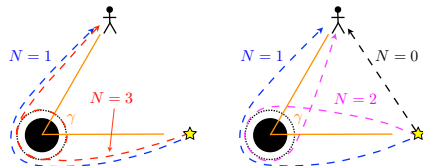
The evolution for a **nonrotating** black hole.

Arrival times

Infinitely many null geodesics connect the source and the observer due to **trapping at the photon sphere**.

The arrival times of the echoes agree with **revolution** around the photon sphere.

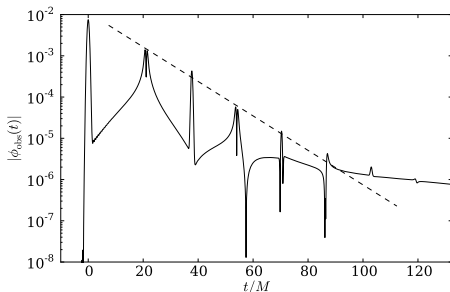
$$T_{\text{full}} = 2\pi\sqrt{27}M \approx 32.648M.$$



Exponential decay

The amplitude decays with the **Lyapunov exponent** of the unstable null geodesics.

$$\lambda = \frac{1}{2\sqrt{27}M} \approx 0.096M^{-1}.$$



These two properties agree with the large ℓ limit of QNMs.

$$\omega \sim \frac{1}{2\sqrt{27}M} (1 - i).$$

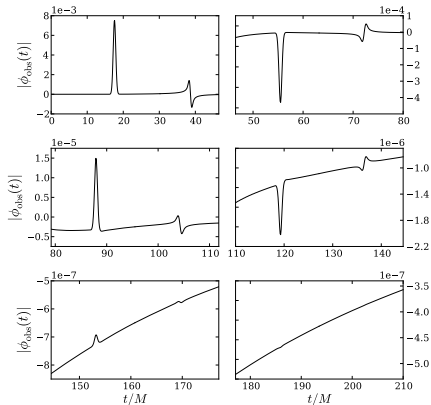


Profiles and the four-fold structure (Ori 2009)

Each caustic passage induces a shift of $\pi/2$ in the profile of the signal.

This effect has been known as the **Gouy phase shift** (1890) in optics, or as the **Hilbert transform** in signal processing.

The recently discovered four-fold structure has a simple explanation: trapping at the photon sphere and Hilbert transform through caustics.



Rotating black holes

The metric includes an additional parameter a , called specific angular momentum. New features are observed in a **rotating** black hole spacetime:

- Frame dragging (Lense–Thirring effect).
- Trapping along spherical photon orbits.
- Singularity structure (?).
- Superradiance (?).
- Extremal case (?).



Possible astrophysical implications (Kocsis 2013)

Ground-based GW detectors will not be sensitive to supermassive black holes because the characteristic frequencies are below the sensitivity bands.

However, GW echoes of inspiraling stellar mass binaries could be measurable. These would come with a delay of a few minutes to hours in galactic nuclei.

The lensed primary signal and GW echo would be amplified if the binary is within a narrow cone behind the supermassive black hole.

⇒ Numerical study of a mathematical question could **expand the science goal** of ground-based GW detectors.



Quasinormal modes along hyperboloidal slices (Schmidt 1993)

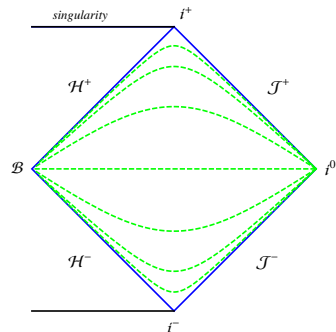
AZ, Physical Review D 2011.

Schwarzschild slices extend between bifurcation sphere and spatial infinity, **but**

- an astrophysical black hole does not possess a bifurcation sphere, and
- idealized observers of radiation are not at spatial infinity.

Perform computations along spacelike surfaces that extend between the future event horizon (**horizon-penetrating**) and future null infinity (**hyperboloidal**).

See also talk by Piotr and Warnick 2013.



Quasinormal modes along hyperboloidal slices (Schmidt 1993)

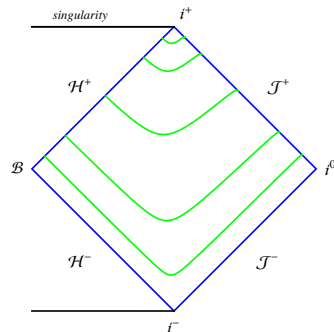
AZ, Physical Review D 2011.

Schwarzschild slices extend between bifurcation sphere and spatial infinity, **but**

- an astrophysical black hole does not possess a bifurcation sphere, and
- idealized observers of radiation are not at spatial infinity.

Perform computations along spacelike surfaces that extend between the future event horizon (**horizon-penetrating**) and future null infinity (**hyperboloidal**).

See also talk by Piotr and Warnick 2013.



Regge–Wheeler equation

Odd-parity gravitational perturbations Ψ satisfy the Regge–Wheeler equation

$$\left[\frac{d^2}{dr_*^2} + \omega^2 - U \right] \Psi = 0, \quad \text{where} \quad f = 1 - \frac{2M}{r}, \quad U = \frac{f}{r^2} \left(\ell(\ell + 1) - \frac{6M}{r} \right).$$

Solutions have the asymptotic behavior

$$\Psi \rightarrow C_1 e^{i\omega r_*} + C_2 e^{-i\omega r_*} \quad \text{as} \quad r_* \rightarrow \pm\infty.$$

The QNM eigenfunctions blow up near the black hole and at infinity.

⇒ The representation of physical boundary conditions becomes unphysical!



Horizon-penetrating, hyperboloidal time functions

Introduce a new time function τ by

$$\tau = t - h(r_*), \quad \text{with} \quad \lim_{r_* \rightarrow \pm\infty} h = \pm r_*.$$

The time transformation amounts to a rescaling

$$\Psi = e^{i\omega h} \psi.$$

The transformed equation becomes an advection-diffusion-reaction equation

$$\left(\frac{d^2}{dr_*^2} + 2i\omega h' \frac{d}{dr_*} + \omega^2(1 - h'^2) + i\omega h'' - U \right) \psi = 0.$$

The asymptotic behavior is regular

$$\psi \rightarrow C_1 + C_2 e^{\mp 2i\omega r_*} \quad \text{as} \quad r_* \rightarrow \pm\infty.$$

This framework leads to efficient numerical computations in time domain.



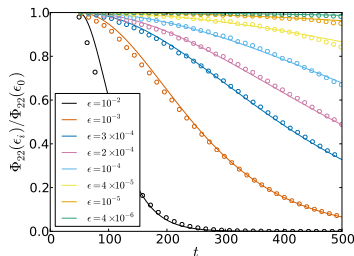
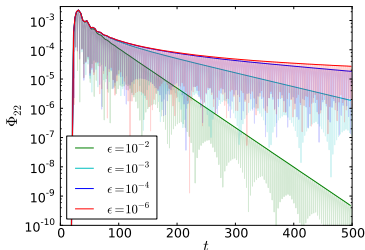
Hyperboloidal evolution in extremal Kerr spacetimes

H Yang, A Zimmerman, AZ, F Zhang, E Berti, Y Chen, *Physical Review D* 2013.

The collective excitation of many weakly damped overtones results in a perturbation that decays as $1/t$ (Glampedakis & Anderson 2001).

The asymptotic scalar field behaves as

$$\Phi_{22}(t; \epsilon) \approx \sqrt{\epsilon} \frac{e^{-\sqrt{\epsilon/8}t}}{1 - e^{-\sqrt{\epsilon/2}t}}, \quad \text{where } \epsilon \equiv 1 - a.$$



Summary

Introduction

Hyperboloidal surfaces

Advantages

Energy decay; Outer boundary; Asymptotic solution; Negative cost

Cubic wave equation

Scalar Green functions

Quasi-normal modes



Thank You!

